Accepted Manuscript

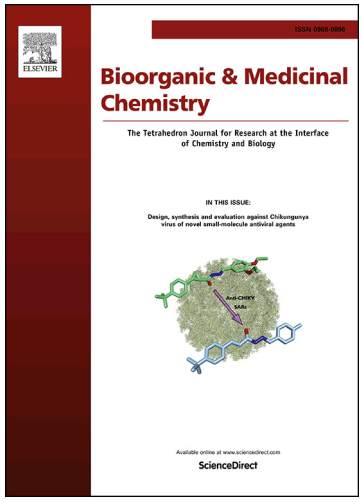

Novel quinazoline derivatives bearing various 6-benzamide moieties as highly selective and potent EGFR inhibitors

Weijie Hou, Yan Ren, Zhenhua Zhang, Huan Sun, Yongfen Ma, Bo Yan

PII: S0968-0896(17)32202-2
DOI: https://doi.org/10.1016/j.bmc.2018.02.022
Reference: BMC 14208

To appear in: *Bioorganic & Medicinal Chemistry*

Received Date: 11 November 2017
Revised Date: 11 February 2018
Accepted Date: 15 February 2018

Please cite this article as: Hou, W., Ren, Y., Zhang, Z., Sun, H., Ma, Y., Yan, B., Novel quinazoline derivatives bearing various 6-benzamide moieties as highly selective and potent EGFR inhibitors, *Bioorganic & Medicinal Chemistry* (2018), doi: https://doi.org/10.1016/j.bmc.2018.02.022

Graphical Abstract

To create your abstract, type over the instructions in the template box below.
Fonts or abstract dimensions should not be changed or altered.

Novel quinazoline derivatives bearing various 6-benzamide moieties as highly selective and potent EGFR inhibitors

Leave this area blank for abstract info.

Weijie Hou*, Yan Ren, Zhenhua Zhang, Huan Sun, Yongfen Ma, Bo Yan
7 Science Park Rd. ZGC Life Science Park, Beijing

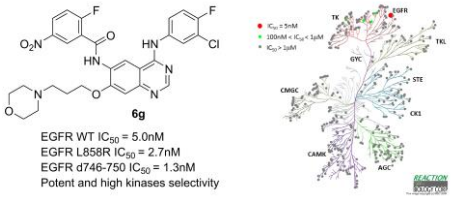

Bioorganic & Medicinal Chemistry
journal homepage: www.elsevier.com

Novel quinazoline derivatives bearing various 6-benzamide moieties as highly selective and potent EGFR inhibitors

Weijie Hou[a,b,*], Yan Ren[b], Zhenhua Zhang[c], Huan Sun[b], Yongfen Ma[b], Bo Yan[b]

[a] *College of Life Sciences, Beijing Normal University, Beijing 100875, China*
[b] *National Institute of Biological Sciences (NIBS), Beijing 102206, China*
[c] *Beijing Advanced Innovation Center for Food Nutrition and Human Health, Department of Applied Chemistry, China Agricultural University, Beijing 100193, China*

ARTICLE INFO

Article history:
Received
Received in revised form
Accepted
Available online

Keywords:
EGFR
Kinase inhibitor
Quinazoline
High selectivity
Anti-cancer

ABSTRACT

A series of novel quinazoline derivatives bearing various C-6 benzamide substituents were synthesized and evaluated as EGFR inhibitors, and most showed significant inhibitory potency against EGFR kinase. In particular, compound **6g** possessed potent inhibitory activity against EGFR wild-type (IC_{50} = 5 nM), and strong antiproliferative activity against HCC827 and Ba/F3 (L858R) cell lines. Kinase profiling against a panel of 365 kinases showed that **6g** was highly selective for EGFR. Furthermore, **6g** showed desirable properties in assays of liver microsome metabolic stability and cytochromes P450 inhibition and preliminary pharmacokinetic study. The overall attractive profile of **6g** made it an interesting compound for further development.

1. Introduction

Epidermal growth factor receptor (EGFR) is a receptor tyrosine kinase (RTK) of the ErbB family.[1] EGFR is known to be a key regulator of many complex biological processes, including cell motility, adhesion, and cell cycle regulation, as well as angiogenesis, apoptosis, and metastasis.[2, 3] Aberrant activity of EGFR has been observed in a wide variety of human cancers,[4] such as non-small cell lung cancer (NSCLC),[5] head and neck cancer,[6] breast cancer,[7] and colorectal cancer,[8] and the dysregulation of EGFR signaling is invariably associated with poor clinical outcomes.[2] Based on its critical role in the tumor progression, many antibodies and small molecule inhibitors that target EGFR have been developed over the last three decades. Several of them (*e.g.*, gefitinib[9, 10] and erlotinib,[11, 12]) have been approved by the US Food and Drug Administration (FDA).

However, the dramatic efficacy of gefitinib and erlotinib for the treatment of NSCLC patients that harbor EGFR mutations, L858R or delE746_A750,[13] is threatened by drug resistance.[14, 15, 16] A secondary mutation T790M in the gatekeeper of EGFR kinase domain accounts for about half of all known cases of acquired resistance to gefitinib or erlotinib.[15, 17] Irreversible inhibitors of EGFR have been demonstrated as an effective tactic for overcoming drug resistance that is driven by the T790M mutation.[18, 19, 20, 21] To date, several irreversible inhibitors have been approved, including afatinib,[22] osimertinib,[23] and olmutinib.[24]

Most irreversible EGFR inhibitors reported to date use acrylamide fragment to react with the Cys797 within the EGFR ATP-binding pocket.[25, 26] It has been reported that the intrinsic reactivity of acrylamide fragment can cause rapid metabolic deactivation, toxicity or nonspecific reactions with off-target biomolecules.[26, 27] Some other cysteine-reactive warheads have been explored in the course of covalent EGFR inhibitor development efforts, (*e.g.*, butynamide, vinylsulfonamide, α-substituted acetamide, alkynyl thienopirimidine),[25] but more systematic studies about application of different covalent groups in EGFR inhibitors are required to provide more information about further optimization of the efficacy/toxicity ratio.

2. Compound design

Phenyl with leaving groups (LGs) and electron withdrawing groups (EWGs) can be viewed as a potential cysteine-reactive group. In 1945, Frederick Sanger used 1-fluoro-2,4-dinitrobenzene(DNFB) to determine the identity of N-terminal amino acid residues in polypeptide chains.[28] In 2012, Merck reported a novel class of HCV NS5B polymerase covalent inhibitors that contained *p*-fluoro-nitrophenyl as the cysteine acceptor: the fluoro atom is used as the LG and the nitro group is used as the EWG.[29] Thus, the reactivity of this type of functional

* Corresponding author. Tel.: +86-010-80726688-8577; fax: +86-010-80705587; e-mail: houweijie@nibs.ac.cn

group can be finely adjusted by using different LGs and EWGs. Importantly, LGs and EWGs can be placed at different phenyl positions, offering considerable structural flexibility.

Here, we performed molecular docking simulation to help better understand if these functional groups could be used to develop EGFR inhibitors with a quinazoline scaffold. We employed a known crystal structure of EGFR T790M (PDB ID: 4G5P)[30] to model the binding mode of the quinazoline compound with a benzamide moiety at the C-6 position (named as **6a** below) (Fig. 1). A highly conserved hydrogen bond was predicted between the quinazoline ring N-1 and Met793 in the EGFR hinge region, and the 4-aniline moiety protrudes into the hydrophobic pocket of EGFR. The benzamide moiety occupies the sugar region of the ATP-binding pocket. The carbon atoms at the *ortho*- and *meta*-positions of benzamide could readily reach (within 5Å) the sulfhydryl group of the Cys797 residue of EGFR where they are ready for nucleophilic attack. Based on the docking result, a series of novel quinazoline derivatives bearing this new functional covalent group were synthesized.

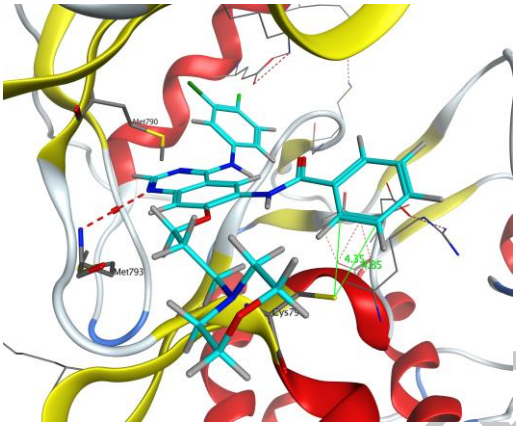

Figure 1. Putative binding mode of **6a** within the ATP-binding pocket of EGFR T790M (PDB ID: 4G5P).

3. Results and discussion

3.1. Synthesis

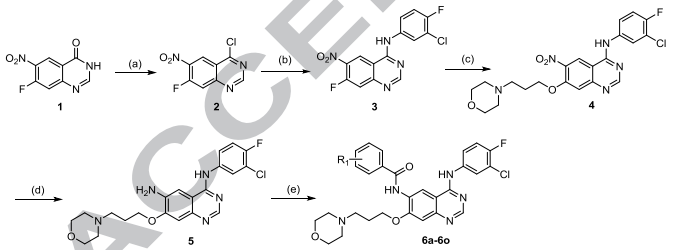

Scheme 1. Synthesis of analogs **6a-o**. Reagents and conditions: (a) $SOCl_2$/cat. DMF, reflux; (b) 3-chloro-4-fluoroaniline, i-PrOH, 90°C; (c) 3-morpholinopropan-1-ol, t-BuOK, t-BuOH/THF, 0°C to rt; (d) Fe, NH_4Cl, EtOH /H_2O, 80°C; (e) aromatic acid, oxalyl chloride/cat. DMF, DCM, 0°C to rt; THF, TEA, 0°C.

The analogs **6a-o** were prepared by using 7-fluoro-6-nitroquinazolin-4(3H)-one (**1**) as the starting material (Scheme 1). Briefly, **2** was obtained through chlorination with thionyl chloride, and then reacted with 3-chloro-4-fluoroaniline to produce **3**. The C-7 position of quinazoline in **3** was substituted with 3-morpholinopropan-1-ol to afford the intermediate **4**, and reduction of the nitro group in **4** with iron power/ammonium chloride yielded the key intermediate **5**. **5** was reacted with different benzoic acids to obtain analogs **6a-o**. Compound **6p** was prepared via reductive amination of **5** with 2-fluoro-5-nitrobenzaldehyde. The synthetic route of analogs **9a-i** is shown in Scheme S1 (Supplementary data-1). Intermediate **3** was reacted with different aliphatic alcohols, and then nitro group reduction and amidation reactions according to Scheme **1** were used to yield the title compounds. The synthesis of analogs **13a-j** are illustrated in Scheme S2 (Supplementary data-1). Intermediate **2** was reacted with different aromatic aniline and went through the next three steps according to Scheme 1 (steps c, d, and e) to obtain the analogs **13a-j**.

3.2. Biological activity

*3.2.1. Biological activity of **6a-p***

Table 1.

In vitro EGFR kinase inhibition activities of **6a-p**

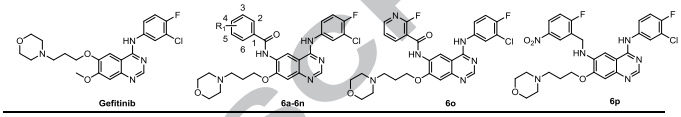

No.	R_1	EGFR WT IC_{50}(nM)	A431 IC_{50}(nM)
Gefitinib	—	0.5	768
6a	H	27	134
6b	2, 3-F, F	29	220
6c	2-F-3-NO_2	13	1100
6d	2-F-3-CF_3	30	>10μM
6e	2-F-3-SO_2Me	24	189
6f	2-Cl-3-NO_2	14	265
6g	2-F-5-NO_2	5.0	2352
6h	2-F-5-CN	1.3	>50μM
6i	2-F-5-SO_2Me	57	396
6j	2-Cl-5-NO_2	8.3	>50μM
6k	5-F-2-NO_2	43	887
6l	2, 3, 5-F, F, F	365	>10μM
6m	2-F	3	146
6n	5-NO_2	50.9	107
6o	—	4.3	66
6p	—	242.4	331

Table 2.

Cell antiproliferative activities of selected compounds

No.	**Gefitinib**	**6c**	**6g**	**6h**	**6j**	**6k**
H1975 IC_{50}(nM)	7184	2480	5340	>50μM	>50μM	2675

We use an HTRF KinEASE-TK kit (Cat# 62TK0PEC) and a Cell Titer-Glo Luminescent Cell Viability Assay kit (Cat# G7573) to test, respectively, kinase inhibition activity and cell antiproliferative activity; the assay results for analogs **6a-p** are summarized in Table 1 and Table 2. With benzamide at the C-6 position of quinazoline (**6a**), the EGFR kinase inhibitory potency (IC_{50}) was 27nM. A fluoro atom was introduced to the phenyl C-2 position as the LG, and different EWGs (fluoro, nitro, trifluoromethyl, and methyl sulfonyl) were introduced the *ortho*-position of this fluoro atom (**6b**-**6e**). Compounds **6b**, **6d**, and **6e** showed the similar inhibitory activity against WT EGFR as did **6a**, while **6c** showed a 2-fold improvement. EWGs were also introduced to the *para*-position of the fluoro atom (**6g**-**6i**), and as compared with **6a**, both **6g** and **6h** showed improved inhibitory activity, **6i** was 2-fold less potent than **6a**, perhaps as a result of steric hindrance by its methyl sulfonyl group. We also explored

using a chloride atom as the LG (compounds **6f** and **6j**), but this change had only very minor effects on inhibitory potency. We examined the use of a fluoro atom as the EWG: we introduced fluoro atom to both *ortho*- and *para*-positions of the LG (fluoro) to obtain **6l**, which was 13-fold less potent than **6a**. When the nitro group of **6g** was removed, **6m** had very similar potency; when the fluoro of **6g** atom was removed, **6n** was about 10-fold less potent than **6g**. Replacement of phenyl ring of **6m** with a pyridine ring to obtain **6o**, and **6o** showed virtually equal potency with **6m**. When benzamide (**6g**) changed to benzylamine (**6p**), a dramatic decrease (about 48-fold) in potency was observed. Based on kinase inhibitory activity data, we selected five compounds to test their antiproliferative activity against the H1975 cell line, and found that compounds **6c**, **6g**, and **6k** showed more potent antiproliferative activity than gefitinib.

*3.2.2. Inhibitory effects of **6g** on EGFR phosphorylation*

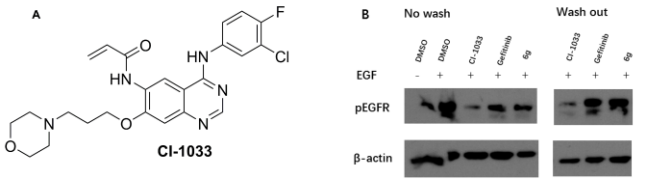

Figure 2. (A) Chemical structure of CI-1033. (B) Inhibition of EGFR autophosphorylation in A431 cells. The treatment concentration of compounds: 10-fold of IC_{50}.

Our bioactivity data did not enable us to determine if these compounds inhibited EGFR in an irreversible manner, so compound **6g** was selected as the representative compound to react with reduced glutathione (GSH)[31] *in vitro* to confirm the reactivity against thiol nucleophiles. The results demonstrated that **6g** could transform into the adduct in the presence of GSH (Fig. S1, S2 and S3, Supplementary data-1). We also compared **6g** with some 2nd (CI-1033 and Afatinib) and 3rd (WZ4002 and Osimertinib) generation EGFR inhibitors against different genotypes EGFR kinases, and **6g** showed less potent kinase activity than these four irreversible inhibitors (Table S5, Supplementary data-1). **6g** was also selected to perform the wash/no wash assays. Western blotting revealed that CI-1033, the positive control and a known irreversible inhibitor of EGFR, inhibited the autophosphorylation of EGFR in both no wash and wash out treatments, while gefitinib (negative control) and **6g** showed no effect in the wash-out treatment (Fig. 2). This result established that **6g** can inhibit the autophosphorylation of EGFR, and does so in a reversible manner, and is thus similar to gefitinib. One explanation for the non-irreversible inhibition that we observed might be that the angle between the carbon atom bearing the fluoro atom at the nitrophenyl and the sulfhydryl group of Cys797 is not conducive for nucleophilic attack to form the covalent bond.

*3.2.3. Kinase profiling of **6g***

Profiling of the activity of compound **6g** against a panel of 365 kinases was conducted, and this analysis indicated that **6g** is highly selective as an EGFR inhibitor (partial results are shown in Table 3 and Table S1, Supplementary data-1; complete results can be found in Supplementary data-2). Using kinase activity inhibition > 80% as the cutoff, **6g** only showed activity against two kinases in the panel: EGFR and DDR1. In clinical patients treated with EGFR drugs, the most common adverse events are skin disorders[32, 33] and diarrhea.[34] These side effects can compromise the patients' quality of life, and can even result in dose-reduction or interruption of treatment.[35] Naoko Yamamoto *et al.* (2011) demonstrated that off-target inhibition of serine/threonine Kinase 10 (STK10) by erlotinib contributes to severe skin disorders.[36] Previously reported inhibition assays of gefitinib and erlotinib (1μM) showed, respectively, 80.8 and 92.7% inhibition of STK10 activity.[37] **6g** (1μM), however, showed only 15.6% inhibition of STK10 activity (Table 2), suggesting that **6g** may be relatively safer and confer fewer adverse effects. Our kinase profiling results demonstrate that modification of the C-6 position of the quinazoline scaffold (the sugar region of the ATP-binding pocket) can improve the kinase selectivity of EGFR inhibitors based on quinazoline, a finding that has been mentioned in several previous reports.[38, 39]

Table 3.

Percent inhibition of compound **6g** at 1 μM against selected kinases[a]

Kinase	Percent inhibition	Kinase	Percent inhibition
DDR1	92.1%	**EGFR**	98.3%
ERBB2/HER2	35.2%	**ERBB4/HER4**	46.7%
EPHA6	76.1%	**MEK5**	79.0%
c-Met	56.9%	**c-MER**	52.8%
LOK/STK10	15.6%		

[a] Compound was tested in single dose duplicate mode, at a concentration of 1 μM. Reactions were carried out at 1 μM ATP. This table includes all the six kinases for which **6g** showed an inhibitory percentage was above 50. Data for the other kinases in the panel can be found in supplementary data-2.

*3.2.4. Biological activity of **9a-i***

Table 4.

In vitro EGFR kinase inhibitory activities (IC_{50}: nM) of analogs **9a-i**

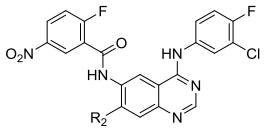

No.	R_2	EGFR WT	EGFR L858R	EGFR d746-750
6g	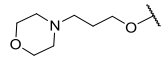	5.0	2.7	1.3
9a	F	44	17	11
9b	OMe	68	74	35
9c	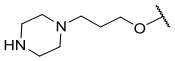	2.6	1.9	0.6
9d	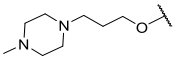	6.6	3.8	3.9
9e	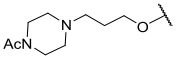	21	14	5.3
9f	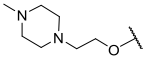	13	12	1.7
9g	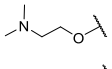	50	18	9.2
9h	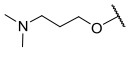	9.2	3.8	3.1
9i	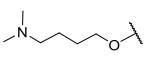	6.3	3.8	ND[a]

[a] ND: not determined.

On the basis of aforementioned results, we decided to pursue the development of potent EGFR inhibitors with high selectivity instead of developing irreversible inhibitors against drug resistance. We conducted an investigation of C-7 substituents of quinazoline (analogs **9a-i**) to identify yet more potent EGFR inhibitors (Table 4). When a fluoro atom was introduced to the C-7 position of quinazoline (**9a**), the potency decreased by about 9-fold compared to **6g**. Compound **9b**, with a methoxy group at the C-7 position, was 13-fold less potent than **6g** in WT EGFR. Several other substituents were also investigated, including piperazine analogs (**9c-f**) and dimethylamine analogs (**9g-i**). When the morpholine group of **6g** was substituted with a piperazine group (**9c**), these two compounds had almost the same potency. When a methyl group was introduced to the 4-positon of the piperazine (**9d**), the potency in WT EGFR decreased slightly. Compound **9e** has an acetyl group at the 4-positon of the piperazine, and was 8-fold less potent than **9c**. Compared to the 3-carbon chain of **9d**, the shorter 2-carbon chain (**9f**) resulted in a slightly decreased potency against WT EGFR. Compared with **9g**, extension of carbon chain, **9h** (3-carbon chain) and **9i** (4-carbon chain) showed a 5-fold and 8-fold improvement, respectively, against WT EGFR.

*3.2.5. Biological activity of **13a-j***

Table 5.

In vitro EGFR kinase inhibitory activities (IC_{50}: nM) of analogs **13a-j**

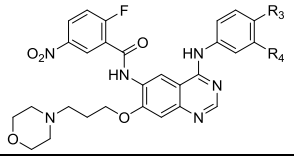

No.	R_3	R_4	EGFR WT	EGFR L858R	EGFR d746-750
6g	F	Cl	5.0	2.7	1.3
13a	F	F	53	32	11
13b	F	H	722	427	110
13c	CN	Cl	2426	2245	474
13d	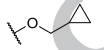	Cl	172	735	71
13e	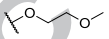	Cl	503	463	210
13f	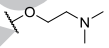	Cl	374	270	128
13g	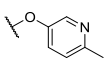	Cl	390	666	419
13h	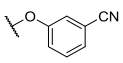	Cl	169	475	268
13i	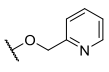	Cl	39	194	125
13j	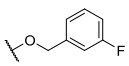	Cl	28	>200	>200

Further exploration at the C-4 position of quinazoline was also conducted to search for a group that was capable of establishing additional interactions with the nearby hydrophobic pocket of EGFR. When the chlorine atom at the *meta*-position of aniline (**6g**) was replaced with a fluoro atom (**13a**), the potency decreased by about 10 folds; a further 10-fold decrease in potency resulted when the fluoro atom was removed (**13b**). The introduction of a cyano group to the *para*-position of aniline (**13c**) resulted in a dramatic drop (at least 485-fold) in potency compared with **6g**. A number of substituents, including small aliphatic and large aromatic groups were investigated in compounds **13d-13j**. With the exception of **13i** and **13j**, these compounds were less potent than **6g**, with IC_{50} values above 150nM; these decreases in potency are likely attributable to unfavorable interactions between these substituents and the hydrophobic pocket of EGFR. Compounds **13i** and **13j** had IC_{50} values of 39nM and 28nM, respectively. Additionally, 14 compounds (Table S2, selected from among **9a-i** and **13a-j)** were evaluated for their antiproliferative activity against the H1975 cell line; and 4 were found to be more potent than gefitinib.

*3.2.6. Evaluation of **6g** against various cell lines*

Table 6.

Cell antiproliferative activity of **6g** against various cell lines

Cell Line	IC_{50} (μM)	Cell Line	IC_{50} (μM)
Ba/F3 (EGFR L858R)	0.182	SF295 (EGFR WT)	>10
Ba/F3 (EGFR Del E746 _A750)	0.178	SF539 (EGFR WT)	>10
HCC827 (EGFR Del E7 46_A750)	0.098	Ba/F3 (cat-EGFR)	>10
A431 (EGFR WT)	2.35	HEK293	>10
NCI-H1975 (EGFR L85 8R/T790M)	5.34	Ba/F3 (Her2 negative)	>10

Compound **6g** was selected for further biological evaluation, and was evaluated against various cell lines that harbored different EGFR mutations and HEK293 (normal human embryonic kidney cells). Compound **6g** showed potent inhibition of the growth of Ba/F3 (EGFR L858R), Ba/F3 (EGFR del E746_A750), and HCC827 cell lines; it did not display obvious antiproliferative activity against the cell lines with WT EGFR (SF295, SF539, Ba/F3) (Table 6). It is known that in patients the concurrent inhibition of WT EGFR by inhibitors can lead to adverse effects, including skin rash and diarrhea.[40, 41] The fact that **6g** has almost no antiproliferative activity against cell lines with WT EGFR implies that it should be able to reduce these adverse effects. The IC_{50} of compound **6g** against HEK293 exceeded 10 μM, indicating that the cytotoxic effects of **6g** appear to be minimal.

*3.2.7. Preliminary druggability evaluation of **6g**.*

Table 7.

Pharmacokinetic parameters of **6g** in mouse[a]

Route	C_{max} (ng/mL)	T_{max} (hr)	AUC_{last} (hr*ng/mL)	AUC_{Inf} (hr*ng/mL)	$T_{1/2}$ (hr)	MRT (hr)	F (%)
Oral	44.2	2.00	563	669	8.77	12.47	57.1

[a] The pharmacokinetic parameters are determined after oral administration of a single (10 mg/kg) dose.

We also evaluated the preliminary druggability of compound **6g**. **6g** was tested for its inhibition of human cytochrome P450 (CYP) enzymes (5 isoforms: 1A2, 2D6, 3A4, 2C9, 2C19) and the IC_{50} values were all higher than 50 μM (Table S3, Supplementary data-1). These results suggest that **6g** has a low potential for involvement in drug-drug interactions. Liver microsome metabolic stability assays were also conducted, and the half-life

of **6g** in human, rat, and mouse all exceeded 90min (Table S4, Supplementary data-1), suggesting that **6g** should have excellent metabolic stability in the liver. A pharmacokinetic study of **6g** was performed in mouse (Table 7): **6g** demonstrated fair oral bioavailability (57.1%) and a desirable half-life time (8.77h). It is known that nitro-anion radical or a nitroso group could form as a result of the reduction of nitro group.[29, 42] So we performed the *Salmonella*/mammalian microsome Mini-AMES reverse mutation assay[43] to evaluate this potential safety issues of compound **6g**. No bacterial mutagenicity was observed under the tested doses in TA98 strain with or without metabolic activation (Table S6, Supplementary data-1); while **6g** showed bactericidal effect at highest dose in TA100 strain both with and without metabolic activation; no bacterial mutagenicity was observed at the rest doses in TA100 strain with or without metabolic activation (Table S7, Supplementary data-1). The results above demonstrated that little potential safety issues related to nitro group of **6g** has been found in Mini-AMES assay.

4. Conclusion

In summary, a series of 4-amino quinazoline derivatives with C-6 benzamide substituents were synthesized and evaluated as EGFR inhibitors. The representative compound **6g** strongly inhibited the kinase activity of EGFR and displayed potent cancer cell antiproliferative activity, while showing minimal cytotoxicity to HEK293 cell line. Western blotting showed that the phosphorylation of EGFR was inhibited by compound **6g**, and in a reversible manner. Kinase inhibition profiling (with a panel of 365 kinases) for **6g** demonstrated that this compound is a highly selective EGFR inhibitor. Importantly, **6g** performed well in liver microsome metabolic stability and CYP inhibition assays, and showed desirable pharmacokinetic properties. No bacterial mutagenicity was observed with **6g** in *Salmonella*/mammalian microsome Mini-AMES reverse mutation assay. In conclusion, we identified the new quinazoline derivative **6g** with a *p*-nitro-fluoro-benzamide moiety at the C-6 position and demonstrate that this new lead compound is a highly selective inhibitor of EGFR. Further evaluation of this compound's druggability is currently in progress.

5. Experiments

5.1. General

The reagents and solvents for reactions were reagent-grade and used without further purification. Glass apparatus for reaction dewater and deoxygenize under nitrogen atmospheric and high temperature. Reactions sensitive to water and air rigorously followed water-free and oxygen-free reaction procedure, added reagents with injection syringe. LC-MS system: Waters 2545 (XBndgeTM C18) / 3100 Mass Detector. ^{1}H NMR spectra were recorded using a Varian Mercury 400 spectrometer under 400 MHz with tetramethylsilane (TMS) as an internal standard. The NMR data are given as follows: chemical shift (δ) in ppm, coupling constants (*J*) in Hz. ^{13}C NMR were recorded using a Varian Mercury 400 spectrometer under 100 MHz. Data of ^{1}H NMR are reported as follows: chemical shift, multiplicity (s = singlet, br = broad, d = doublet, t = triplet, m = multiplet), coupling constants and integration. High-resolution mass spectra were obtained using Agilent Technolodies 6540 UHD Accurate-Mass Q-TOF LC/MS. Thin-layer chromatography (TLC) was carried out using HS-GF 254 silica plates, Chromatographic purification was carried out using silica gel (Yan tai mou ping yuan bo jing xi silica gel plant)

*5.2. Preparation of compounds **1–5***

Compounds **1-4** were prepared following the Patent: US2003/158408 A1, 2003. Compound **4** (414mg, 0.9mmol) was dissolved in ethanol (4 mL) and water (2mL). Iron powder (251mg, 4.5mmol) and ammonium chloride (240mg, 4.5mmol) were then added, and the resulting mixture was heated to 80°C for 3 hours. The reaction mixture was cooled to room temperature and filtered through celite. The ethanol was removed in vacuo, and the resulting residue was basified with saturated sodium bicarbonate and extracted with ethyl acetate three times. The organic layer was separated and dried using anhydrous sodium sulfate, concentrated to afford 324mg of yellow solid (84%).^{1}H NMR (400 MHz, DMSO-d_6) □ 2.01 (m, 2H), 2.42 (m, 4H), 2.49 (t, *J* =8.4 Hz, 2H), 3.66 (m, 4H), 4.16 (t, *J* = 6.6Hz, 2H), 4.21 (m, 2H), 6.86 (s, 1H), 6.98 (m, 1H), 7.08 (t, *J* = 8.4Hz, 1H), 7.11 (s, 1H), 7.43 (m, 1H), 7.86 (dd, *J* = 2.4, 6.6Hz, 1H), 8.51 (s, 1H).

*5.3. General method for preparing of analogs 6**a-o***

Analogs **6a-o** were synthesized as outlined in Scheme 1: Acid (1.2eq) was dissolved in anhydrous DCM, oxalyl chloride (1.44eq) was added dropwise at 0°C and then one drop DMF was added. The reaction mixture stirred at room temperature for 2 hours. The excess oxalyl chloride was removed under reduced pressure, and the residue dissolved in THF for next transformation.

Intermediate **5** (1eq) and triethylamine (1.5eq) were added sequent to a 25ml three-neck-bottom flask under a nitrogen atmosphere. Acyl chloride in THF was added dropwise to flask at 0°C. The reaction mixture was stirred at 0°C. After pale yellow solid appeared, the mixture reacted at room temperature until TLC showed **5** disappeared. Ice water was added to reaction mixture at 0°C, and stirred for another 30min until no insoluble solid generated. The solid was filtered to get crude product. The crude product further purified by medium pressure column chromatography (C18 padding, ACN: H_2O (containing 0.05% TFA) =1: 99 – 99: 1) to get product as a solid.

*5.3.1. N-(4-((3-chloro-4-fluorophenyl) amino)-7-(3-morpholinop ropoxy) quinazolin-6-yl) benzamide (**6a**)*

Pale yellow solid; yield: 48%.^{1}H NMR (400 MHz, DMSO-d_6) δ 2.22-2.27 (m, 2H), 2.98-3.05 (m, 2H), 3.32-3.36 (m, 2H), 3.43-3.46 (m, 2H), 4.02 (m, 2H), 3.63 (t, *J* = 12.0Hz, 2H), 3.93-3.97 (m, 2H), 4.34 (t, *J* = 5.6Hz, 2H), 7.39 (s, 1H), 7.50 (t, *J* = 9.2Hz, 1H), 7.57-7.62 (m, 2H), 7.64-7.68 (m, 1H), 7.76-7.80 (m, 1H), 8.04-8.07 (m, 2H), 8.12 (dd, *J* = 2.8, 6.8Hz, 1H), 8.75 (s, 1H), 8.89 (s, 1H), 9.82(br, 1H), 10.00 (s, 1H). MS (ESI) m/z = 536.1879 ($M+H^+$), calcd. for $C_{28}H_{27}ClFN_5O_3$ m/z = 536.1865.

*5.3.2. N-(4-((3-chloro-4-fluorophenyl)amino)-7-(3-morpholinopr opoxy)quinazolin-6-yl)-2,3-difluorobenzamide (**6b**)*

Pale yellow solid; yield: 35%. ^{1}H NMR (400 MHz, DMSO-d_6) δ 2.26-2.33 (m, 2H), 3.06-3.12 (m, 2H), 3.38-3.43 (m, 2H), 3.47-3.52 (m, 2H), 3.69-3.76 (m, 2H), 3.96-4.03 (m, 2H), 4.38 (t, *J* = 5.6Hz, 2H), 7.40-7.45 (m, 2H), 7.51 (t, *J* = 9.2Hz, 1H), 7.64-7.77 (m, 3H), 8.05-8.08 (m, 1H), 8.78 (s, 1H), 9.10 (s, 1H), 10.12 (m, 1H), 10.75 (br, 1H). MS (ESI) m/z = 572.1673 ($M+H^+$), calcd. for $C_{28}H_{26}ClF_3N_5O_3$ m/z = 572.1676.

*5.3.3. N-(4-((3-chloro-4-fluorophenyl)amino)-7-(3-morpholinopr opoxy)quinazolin-6-yl)-2-fluoro-3-nitrobenzamide (**6c**)*

Pale yellow solid; yield: 31%. ^{1}H NMR (400 MHz, DMSO-d_6) δ 2.23-2.28 (m, 2H), 3.04-3.13 (m, 4H), 3.64-3.70 (m, 2H), 3.99-4.02 (m, 2H), 4.37 (t, *J* = 5.6Hz, 2H), 7.38 (s, 1H), 7.50 (t, *J* = 9.2Hz, 1H), 7.64 (t, *J* = 8.0Hz, 1H), 7.74-7.77 (m, 1H), 8.08-8.11 (m, 1H), 8.16 (t, *J* = 6.8Hz, 1H), 8.38 (t, *J* = 7.6Hz, 1H), 8.72 (s,

1H), 9.02 (s, 1H), 9.80 (br, 1H), 10.28 (s, 1H). MS (ESI) m/z = 599.1618 ($M+H^+$), calcd. for $C_{28}H_{26}ClF_2N_6O_5$ m/z = 599.1621.

*5.3.4. N-(4-((3-chloro-4-fluorophenyl)amino)-7-(3-morpholinopropoxy)quinazolin-6-yl)-2-fluoro-3-(trifluoromethyl)benzamide (**6d**)*

Pale yellow solid; yield: 40%. ^{1}H NMR (400 MHz, DMSO-d_6) δ 2.23-2.29 (m, 2H), 2.95-3.11 (m, 4H), 3.64-3.72 (m, 2H), 3.97-4.01 (m, 2H), 4.37 (t, *J* = 5.6Hz, 2H), 7.37-7.39 (m, 1H), 7.45-7.51 (m, 1H), 7.62 (t, *J* = 7.6Hz, 1H), 7.76-7.80 (m, 1H), 8.04 (t, *J* = 7.6Hz, 1H), 8.09-8.13 (m, 1H), 8.68 (s, 1H), 8.97 (s, 1H), 10.23 (s, 1H). MS (ESI) m/z = 622.1650 ($M+H^+$), calcd. for $C_{29}H_{26}ClF_5N_5O_3$ m/z = 622.1644.

*5.3.5. N-(4-((3-chloro-4-fluorophenyl)amino)-7-(3-morpholinopropoxy)quinazolin-6-yl)-2-fluoro-3-(methylsulfonyl)benzamide (**6e**)*

Pale yellow solid; yield: 36%. ^{1}H NMR (400 MHz, DMSO-d_6) δ 2.27-2.33 (m, 2H), 3.11 (bs, 2H), 3.38-3.43 (m, 4H), 3.44 (s, 3H), 3.68-3.74 (m, 2H), 3.99-4.03 (m, 2H), 4.38 (t, *J* = 5.6Hz, 2H), 7.43 (s, 1H), 7.50 (t, *J* = 9.2Hz, 1H), 7.66 (t, *J* = 8.0Hz, 1H), 7.74-7.78 (m, 1H), 8.07-8.12 (m, 2H), 8.14-8.18 (m, 1H), 8.76 (s, 1H), 9.06 (s, 1H), 10.10 (br, 1H), 10.31 (d, *J* = 3.2Hz, 1H). MS (ESI) m/z = 632.1545 ($M+H^+$), calcd. for $C_{29}H_{29}ClF_2N_5O_5S$ m/z = 632.1546.

*5.3.6. N-(4-((3-chloro-4-fluorophenyl)amino)-7-(3-morpholinopropoxy)quinazolin-6-yl)-2-chloro-3-nitrobenzamide (**6f**)*

Pale yellow solid; yield: 35%. ^{1}H NMR (400 MHz, DMSO-d_6) δ 2.23-2.29 (m, 2H), 3.02-3.09 (m, 2H), 3.34-3.38 (m, 2H), 3.44-3.48 (m, 2H), 3.65-3.72 (m, 2H), 3.98-4.01 (m, 2H), 4.35 (t, *J* = 5.6Hz, 2H), 7.40 (s, 1H), 7.51 (t, *J* = 9.2Hz, 1H), 7.72-7.76 (m, 1H), 7.77 (t, *J* = 8.0Hz, 1H), 7.94 (dd, *J* = 2.0, 8.0Hz, 1H), 8.05-8.07 (m, 1H), 8.20 (dd, *J* = 2.0, 8.4Hz, 1H), 8.77 (s, 1H), 8.98 (s, 1H), 10.09 (br, 1H), 10.47 (s, 1H). MS (ESI) m/z = 615.1332 ($M+H^+$), calcd. for $C_{28}H_{26}Cl_2FN_6O_5$ m/z = 615.1326.

*5.3.7. N-(4-((3-chloro-4-fluorophenyl)amino)-7-(3-morpholinopropoxy)quinazolin-6-yl)-2-fluoro-5-nitrobenzamide (**6g**)*

Pale yellow solid; yield: 32%. ^{1}H NMR (400 MHz, DMSO-d_6) δ 1.98-2.02 (m, 2H), 2.37 (bs, 4H), 3.28-3.31 (m, 2H), 3.57 (bs, 4H), 4.29 (t, *J* = 5.6Hz, 2H), 7.34 (s, 1H), 7.44 (t, *J* = 9.2Hz, 1H), 7.75 (t, *J* = 9.2Hz, 1H), 7.80-7.84 (m, 1H), 8.15 (dd, *J* = 2.4, 6.8Hz, 1H), 8.52 (m, 1H), 8.58 (s, 1H), 8.60-8.64 (m, 1H), 8.91 (s, 1H), 9.90 (s, 1H), 10.17 (br, 1H). ^{13}CNMR (100 MHz, DMSO-*d6*) δ 25.57, 53.31, 54.59, 66.17, 67.08, 107.55, 108.74, 116.45, 117.31, 118.59, 122.48, 123.63, 124.29, 126.07, 126.39, 128.71, 136.70, 144.00, 149.80, 152.01, 154.36, 155.19, 156.92, 160.44, 161.43, 164.00. MS (ESI) m/z = 599.1627 ($M+H^+$), calcd. for $C_{28}H_{26}ClF_2N_6O_5$ m/z = 599.1621.

*5.3.8. N-(4-((3-chloro-4-fluorophenyl)amino)-7-(3-morpholinopropoxy)quinazolin-6-yl)-2-fluoro-5-cyanobenzamide (**6h**)*

Pale yellow solid; yield: 41%. ^{1}H NMR (400 MHz, DMSO-d_6) δ 2.23-2.29 (m, 2H), 2.43-2.46 (m, 2H), 3.05-3.12 (m, 4H), 3.65-3.71 (m, 2H), 3.99-4.03 (m, 2H), 4.37 (t, *J* = 5.6Hz, 2H), 7.39 (s, 1H), 7.50 (t, *J* = 9.2Hz, 1H), 7.68-7.73 (m, 1H), 7.74-7.78 (m, 1H), 8.08 (dd, *J* = 2.4, 6.4Hz, 1H), 8.18-8.22 (m, 1H), 8.30 (dd, *J* = 2.4, 6.4Hz, 1H), 8.72 (s, 1H), 9.02 (s, 1H), 9.89 (br, 1H), 10.19 (d, *J* = 3.2Hz, 1H). MS (ESI) m/z = 579.1720 ($M+H^+$), calcd. for $C_{29}H_{26}ClF_2N_6O_3$ m/z = 579.1723.

*5.3.9. N-(4-((3-chloro-4-fluorophenyl)amino)-7-(3-morpholinopropoxy)quinazolin-6-yl)-2-fluoro-5-(methylsulfonyl)benzamide (**6i**)*

Pale yellow solid; yield: 28%. ^{1}H NMR (400 MHz, DMSO-d_6) δ 2.25-2.31 (m, 2H), 3.07-3.13 (m, 4H), 3.34 (s, 3H), 3.64-3.71 (m, 4H), 3.99-4.04 (m, 2H), 4.38 (t, *J* = 5.6Hz, 2H), 7.40 (s, 1H), 7.50 (t, *J* = 9.2Hz, 1H), 7.73-7.78 (m, 2H), 8.08 (dd, *J* = 2.8, 6.8Hz, 1H),, 8.22-8.26 (m, 1H), 8.34 (dd, *J* = 2.4, 6.4Hz, 1H), 8.75 (s, 1H), 9.03 (s, 1H), 10.26 (s, 1H). MS (ESI) m/z = 632.1545 ($M+H^+$), calcd. for $C_{29}H_{29}ClF_2N_5O_5S$ m/z = 632.1546.

*5.3.10. N-(4-((3-chloro-4-fluorophenyl)amino)-7-(3-morpholinopropoxy)quinazolin-6-yl)-2-chloro-5-nitrobenzamide (**6j**)*

Pale yellow solid; yield: 36%. ^{1}H NMR (400 MHz, DMSO-d_6) δ 2.21-2.28 (m, 2H), 3.06 (br, 4H), 3.61-3.67 (m, 4H), 3.97-4.00 (m, 2H), 4.36 (t, *J* = 6.0Hz, 2H), 7.39 (s, 1H), 7.51 (t, *J* = 9.2Hz, 1H), 7.73-7.77 (m, 1H), 7.95 (d, *J* = 8.8Hz, 1H), 8.08 (dd, *J* = 2.8, 6.8Hz, 1H), 8.40 (dd, *J* = 2.8, 8.8Hz, 1H), 8.46 (d, *J* = 2.4Hz, 1H), 8.76 (s, 1H), 8.95 (s, 1H), 9.77 (br, 1H), 10.48 (s, 1H). MS (ESI) m/z = 615.1326 ($M+H^+$), calcd. for $C_{28}H_{26}Cl_2FN_6O_5$ m/z = 615.1326.

*5.3.11. N-(4-((3-chloro-4-fluorophenyl)amino)-7-(3-morpholinopropoxy)quinazolin-6-yl)-5-fluoro-2-nitrobenzamide (**6k**)*

Pale yellow solid; yield: 28%. ^{1}H NMR (400 MHz, DMSO-d_6) δ 1.93-2.00 (m, 2H), 2.35 (m, 4H), 2.45 (bs, 4H), 2.46 (t, *J* = 7.2Hz, 2H), 3.56 (t, *J* = 4.4Hz, 4H), 4.26 (t, *J* = 6.4Hz, 2H), 7.32 (s, 1H), 7.44 (t, *J* = 9.2Hz, 1H), 7.62-7.68 (m, 2H), 7.71-7.73 (m, 1H), 7.78-7.82 (m, 1H), 8.12 (dd, *J* = 2.4, 6.8Hz, 1H), 8.31 (dd, *J* = 4.8, 8.8Hz, 1H), 8.55 (s, 1H), 8.82 (s, 1H), 9.96 (s, 1H), 10.30 (s, 1H). MS (ESI) m/z = 599.1627 ($M+H^+$), calcd. for $C_{28}H_{26}ClF_2N_6O_5$ m/z = 599.1621.

*5.3.12. N-(4-((3-chloro-4-fluorophenyl)amino)-7-(3-morpholinopropoxy)quinazolin-6-yl)-2,3,5-trifluorobenzamide (**6l**)*

Pale yellow solid; yield: 40%. ^{1}H NMR (400 MHz, DMSO-d_6) δ 2.24-2.31 (m, 2H), 3.02-3.13 (m, 2H), 3.37-3.41 (m, 4H), 3.69-3.73 (m, 2H), 3.96-4.02 (m, 2H), 4.37 (t, *J* = 5.6Hz, 2H), 7.40-7.41 (m, 1H), 7.47-7.52 (m, 2H), 7.74-7.78 (m, 1H), 7.83-7.90 (m, 1H), 8.09 (dd, *J* = 2.4, 7.6Hz, 1H), 8.71 (s, 1H), 9.02 (s, 1H), 10.17-10.19 (m, 1H), 10.50 (s, 1H). MS (ESI) m/z= 590.1588 ($M+H^+$), calcd. for $C_{28}H_{25}ClF_4N_5O_3$ m/z = 590.1582.

*5.3.13. N-(4-((3-chloro-4-fluorophenyl)amino)-7-(3-morpholinopropoxy)quinazolin-6-yl)-2-fluorobenzamide (**6m**)*

Pale yellow solid; yield: 30%. ^{1}H NMR (400 MHz, DMSO-d_6) δ 2.27-2.32 (m, 2H), 3.05-3.12 (m, 4H), 3.64-3.72 (m, 4H), 4.00-4.04 (m, 2H), 4.38 (t, *J* = 5.6Hz, 2H), 7.39 (s, 1H), 7.41-7.53 (m, 3H), 7.67-7.76 (m, 3H), 7.91 (t, *J* = 7.6Hz, 1H), 8.07 (dd, *J* = 2.4, 6.4Hz, 1H), 8.75 (s, 1H), 9.13 (s, 1H), 9.96 (d, *J* = 6.4Hz, 1H). MS (ESI) m/z = 554.1766 ($M+H^+$), calcd. for $C_{28}H_{27}ClF_2N_5O_3$ m/z = 554.1770.

*5.3.14. N-(4-((3-chloro-4-fluorophenyl)amino)-7-(3-morpholinopropoxy)quinazolin-6-yl)-3-nitrobenzamide (**6n**)*

Pale yellow solid; yield: 30%. ^{1}H NMR (400 MHz, DMSO-d_6) □ 2.19-2.25 (m, 2H), 3.04 (bs, 4H), 3.55-3.65 (m, 4H), 3.94-3.97 δ (m, 2H), 4.35 (t, *J* = 5.6Hz, 2H), 7.39 (s, 1H), 7.49 (t, *J* = 9.2Hz, 1H), 7.77-7.81 (m, 1H), 7.91 (t, *J* = 8.0Hz, 1H), 8.15 (dd, *J* = 2.8, 6.8Hz, 1H), 8.46-8.53 (m, 2H), 8.72 (s, 1H), 8.81 (s, 1H), 8.88 (t, *J* = 2.0Hz, 1H), 9.64 (br, 1H), 10.46 (s, 1H). MS (ESI) m/z = 581.1716 ($M+H^+$), calcd. for $C_{28}H_{27}ClFN_6O_5$ m/z = 581.1715.

*5.3.15. N-(4-((3-chloro-4-fluorophenyl)amino)-7-(3-morpholinopropoxy)quinazolin-6-yl)-2-fluoronicotinamide (**6o**)*

Pale yellow solid; yield: 32%. ^{1}H NMR (400 MHz, DMSO-d_6) δ 2.25-2.33 (m, 2H), 3.06-3.14 (m, 4H), 3.64-3.71 (m, 4H), 4.00-4.05 (m, 2H), 4.38 (t, *J* = 5.6Hz, 2H), 7.39 (s, 1H), 7.50 (t, *J* = 9.2Hz, 1H), 7.59-7.63 (m, 1H), 7.73-7.77 (m, 1H), 8.07-8.09 (m, 1H), 8.38-8.43 (m, 1H), 8.48-8.49 (m, 1H), 8.74 (s, 1H), 9.10 (s, 1H), 9.86 (br, 1H), 10.14 (d, *J* = 4.8Hz, 1H). MS (ESI) m/z = 555.1718 ($M+H^+$), calcd. for $C_{27}H_{26}ClF_2N_6O_3$ m/z = 555.1723.

*5.3.16. Preparation of compound **6p***

Intermediate **5** (22mg, 0.05mmol), 2-fluoro-5-nitrobenzaldehyde (10mg, 0.06mmol) anhydrous methanol(5ml) and acetic acid (2μl, 0.05mmol) were added sequent to 25ml a

dewatered three-neck-bottom flask under a nitrogen atmosphere. The reaction mixture stirred at 60 ° C for 4 hours. Then $NaBH_3CN$(5mg , 0.08mmol) was added to the mixture at 0°C. The reaction was allowed to warm to room temperature and stirred at room temperature for 2 hours. Saturated sodium carbonate solution (3ml) was added to reaction mixture. The solvent was removed under reduced pressure. The residue was partitioned between dichloromethane and water. The organic layer was washed with brine and dried over Na_2SO_4, the solid was filtered off, and the filtrate was concentrated under reduced pressure to get crude product. The crude product purified by medium pressure column chromatography (C18 padding, ACN: H_2O (containing 0.05% TFA) =1: 99 – 99: 1) to get product as a pale-yellow solid (12mg, yield: 41%).^{1}H NMR (400 MHz, DMSO-d_6) δ 2.27-2.31 (m, 2H), 3.08-3.16 (m, 4H), 3.49-3.54 (m, 4H), 3.64-3.70 (m, 2H), 3.98-4.04 (m, 2H), 4.38 (t, *J* = 5.6Hz, 2H), 4.74 (d, *J* = 6.4Hz, 2H), 6.71 (s, 1H), 7.21 (s, 1H), 7.41 (s, 1H), 7.51 (t, *J* = 9.2Hz, 1H), 7.56-7.63 (m, 2H), 7.94-7.97 (m, 1H), 8.20 (dd, *J* = 2.8, 6.4Hz, 1H), 8.24-8.28 (m, 1H), 8.68 (s, 1H), 9.83 (br, 1H). MS (ESI) m/z = 585.1846 ($M+H^+$), calcd. for $C_{28}H_{28}ClF_2N_6O_4$ m/z = 585.1829.

*5.4. General method for preparing of analogs **9a-i***

The analogs **9** was synthesized from intermediate **3** as shown in scheme S1. In step a, different aliphatic alcohol was used to replace 3-morpholinopropan-1-ol according to scheme 1 to obtain intermediates **7**. The next two steps were according to analogs **6** to obtain analogs **9**.

*5.4.1. N-(4-((3-chloro-4-fluorophenyl)amino)-7-fluoroquinazolin-6-yl)-2-fluoro-5-nitrobenzamide (**9a**)*

Pale yellow solid; yield: 35%. ^{1}H NMR (400 MHz, DMSO-d_6) δ 7.50 (t, *J* = 9.2Hz, 1H), 7.72-7.79 (m, 3H), 8.09 (dd, *J* = 2.8, 6.8Hz, 1H), 8.50-8.54 (m, 1H), 8.59 (dd, *J* = 2.8, 6.0Hz, 1H), 8.76 (s, 1H), 9.03 (d, *J* = 8.0Hz, 1H), 10.61 (br, 1H), 10.95 (s, 1H). MS (ESI) m/z = 474.0586 ($M+H^+$), calcd. for $C_{21}H_{12}ClF_3N_5O_3$ m/z = 474.0581. ^{13}C NMR (100 MHz, DMSO-d_6) δ 104.59, 111.58, 116.80, 118.34, 119.03, 120.62, 123.84, 124.48, 125.10, 125.47, 125.93, 128.74, 135.46, 143.87, 153.00, 153.94, 155.43, 157.65, 159.94, 161.39, 163.95.

*5.4.2. N-(4-((3-chloro-4-fluorophenyl)amino)-7-methoxyquinazolin-6-yl)-2-fluoro-5-nitrobenzamide (**9b**)*

Pale yellow solid; yield: 32%. ^{1}H NMR (400 MHz, DMSO-d_6) δ 4.04 (s, 3H), 7.36 (s, 1H), 7.44 (t, *J* = 9.2Hz, 1H), 7.72 (t, *J* = 9.2Hz, 1H), 7.79-7.83 (m, 1H), 8.14 (dd, *J* = 2.4, 6.8Hz, 1H), 8.48-8.52 (m, 1H), 8.57-8.59 (m, 2H), 8.95 (s, 1H), 9.95 (s, 1H), 10.28 (d, *J* = 3.2Hz, 1H). MS (ESI) m/z = 486.0797 ($M+H^+$), calcd. for $C_{22}H_{15}ClF_2N_5O_4$ m/z = 486.0781.

*5.4.3. N-(4-((3-chloro-4-fluorophenyl)amino)-7-(3-(piperazin-1-yl)propoxy)quinazolin-6-yl)-2-fluoro-5-nitrobenzamide (**9c**)*

Tert-butyl-4-(3-hydroxypropyl)piperazine-1-carboxylate was used in step a and the intermediate got from step b and c went through removal of t-butyloxy carbonyl by TFA to obtain the compound **9c**. ^{1}HNMR (400 MHz, DMSO-d_6) δ 2.11 (m, 2H), 2.92 (m, 4H), 3.23 (m, 4H), 4.34 (t, *J* = 5.6Hz, 2H), 7.38 (s, 1H), 7.50 (t, *J* = 9.2Hz, 1H), 7.73-7.78 (m, 2H), 8.08-8.10 (m, 1H), 8.53-8.56 (m, 1H), 8.61-8.63 (m, 1H), 8.73 (s, 1H), 9.02 (s, 1H), 10.29 (s, 1H), 10.54 (br, 1H). MS (ESI) m/z = 598.1802 ($M+H^+$), calcd. for $C_{28}H_{27}ClF_2N_7O_4$ m/z = 598.1781.

*5.4.4. N-(4-((3-chloro-4-fluorophenyl)amino)-7-(3-(4-methylpiperazin-1-yl)propoxy)quinazolin-6-yl)-2-fluoro-5-nitrobenzamide (**9d**)*

Pale yellow solid; yield: 31%. ^{1}H NMR (400 MHz, DMSO-d_6) δ 2.08-2.14 (bs, 2H), 2.78 (s, 3H), 2.90 (bs, 2H), 3.08 (bs, 2H), 3.20-3.28 (m, 2H), 3.39-3.46 (m, 2H), 4.35 (t, *J* = 5.6Hz, 2H), 7.40-7.42 (m, 1H), 7.53 (t, *J* = 9.2Hz, 1H), 7.71-7.78 (m, 2H), 8.06 (dd, *J* = 2.4, 6.8Hz, 1H), 8.52-8.56 (m, 1H), 8.62 (dd, *J* = 3.2, 6.0Hz, 1H), 8.81 (s, 1H), 9.06 (s, 1H), 10.32 (d, *J* = 4.0Hz, 1H), 10.83 (s, 1H). MS (ESI) m/z = 612.1933 ($M+H^+$), calcd. for $C_{29}H_{29}ClF_2N_7O_4$ m/z = 612.1938.

*5.4.5. N-(7-(3-(4-acetylpiperazin-1-yl)propoxy)-4-((3-chloro-4-fluorophenyl)amino)quinazolin-6-yl)-2-fluoro-5-nitrobenzamide (**9e**)*

Pale yellow solid; yield: 29%. ^{1}H NMR (400 MHz, DMSO-d_6) δ 2.06 (s, 3H), 2.25-2.31 (m, 2H), 2.92-2.98 (m, 2H), 3.06-3.12 (m, 2H), 3.37-3.40 (m, 2H), 3.50-3.56 (m, 2H), 3.99-4.03 (m, 2H), 4.38 (t, *J* = 5.6Hz, 2H), 7.42 (s, 1H), 7.49 (t, *J* = 9.2Hz, 1H), 7.72-7.79 (m, 2H), 8.10 (dd, *J* = 2.8, 6.8Hz, 1H), 8.52-8.56 (m, 1H), 8.64 (dd, *J* = 3.2, 6.0Hz, 1H), 8.71 (s, 1H), 9.03 (s, 1H), 9.93 (br, 1H), 10.28 (d, *J* = 3.6Hz, 1H), 10.47 (br, 1H). MS (ESI) m/z = 640.1900 ($M+H^+$), calcd. for $C_{30}H_{29}ClF_2N_7O_5$ m/z = 640.1887.

*5.4.6. N-(4-((3-chloro-4-fluorophenyl)amino)-7-(2-(4-methylpiperazin-1-yl)ethoxy)quinazolin-6-yl)-2-fluoro-5-nitrobenzamide (**9f**)*

Pale yellow solid; yield: 30%. ^{1}H NMR (400 MHz, DMSO-d_6) δ 2.77 (s, 3H), 3.06 (bs, 4H), 3.22-3.39 (m, 6H), 3.39 (bs, 2H), 4.43 (t, *J* = 4.4Hz, 2H), 7.44 (s, 1H), 7.52 (t, *J* = 9.2Hz, 1H), 7.71-7.78 (m, 2H), 8.07 (dd, *J* = 2.8, 7.2Hz, 1H), 8.53-8.57 (m, 1H), 8.62 (dd, *J* = 2.8, 5.6Hz, 1H), 8.78 (s, 1H), 9.05 (s, 1H), 10.33 (d, *J* = 3.2Hz, 1H), 10.74 (br, 1H). MS (ESI) m/z = 598.1791 ($M+H^+$), calcd. for $C_{28}H_{27}ClF_2N_7O_4$ m/z = 598.1781.

*5.4.7. N-(4-((3-chloro-4-fluorophenyl)amino)-7-(2-(dimethylamino)ethoxy)quinazolin-6-yl)-2-fluoro-5-nitrobenzamide (**9g**)*

Pale yellow solid; yield: 30%. ^{1}H NMR (400 MHz, DMSO-*d6*) δ 2.94 (s, 3H), 2.95 (s, 3H), 3.67 (t, *J* = 4.4Hz, 2H), 4.64 (t, *J* = 4.8Hz, 2H), 7.44 (s, 1H), 7.47 (t, *J* = 9.2Hz, 1H), 7.70 (t, *J* = 9.2Hz, 1H), 7.76-7.80 (m, 1H), 8.11 (dd, *J* =2.8, 6.8Hz, 1H), 8.18-8.22 (m, 1H), 8.32 (dd, *J* = 2.4, 6.8Hz, 1H), 8.66 (s, 1H), 9.02 (s, 1H), 9.56 (br, 1H), 10.14 (s, 1H). LC-MS (ESI) m/z = 543.2 ($M+H^+$), calcd. for $C_{25}H_{22}ClF_2N_6O_4$ m/z = 543.1359.

*5.4.8. N-(4-((3-chloro-4-fluorophenyl)amino)-7-(3-(dimethylamino)propoxy)quinazolin-6-yl)-2-fluoro-5-nitrobenzamide (**9h**)*

Pale yellow solid; yield: 36%. ^{1}H NMR (400 MHz, DMSO-d_6) δ 2.20-2.27 (m, 2H), 2.83 (s, 3H), 2.84 (s, 3H), 3.30-3.35 (m, 2H), 4.36 (t, *J* = 5.6Hz, 2H), 7.38 (s, 1H), 7.48 (t, *J* = 9.2Hz, 1H), 7.73-7.79 (m, 2H), 8.12 (dd, *J* = 2.4, 6.8Hz, 1H), 8.52-8.56 (m, 1H), 8.63 (dd, *J* = 2.8, 6.0Hz, 1H), 8.68 (s, 1H), 8.99 (s, 1H), 9.50 (br, 1H), 10.26 (d, *J* = 3.2Hz, 1H). MS (ESI) m/z = 557.1510 ($M+H^+$), calcd. for $C_{26}H_{24}ClF_2N_6O_4$ m/z = 557.1516.

*5.4.9. N-(4-((3-chloro-4-fluorophenyl)amino)-7-(4-(dimethylamino)butoxy)quinazolin-6-yl)-2-fluoro-5-nitrobenzamide (**9i**)*

Pale yellow solid; yield: 35%. ^{1}H NMR (400 MHz, DMSO-d_6) δ 1.85-1.90 (m, 4H), 2.77 (s, 3H), 2.78 (s, 3H), 3.12-3.17 (m, 2H), 4.31 (t, *J* = 5.2Hz, 2H), 7.38 (s, 1H), 7.48 (t, *J* = 9.2Hz, 1H), 7.72-7.80 (m, 2H), 8.11 (dd, *J* = 2.4, 6.8Hz, 1H), 8.52-8.56 (m, 1H), 8.62 (dd, *J* = 3.2, 6.0Hz, 1H), 8.68 (s, 1H), 8.98 (s, 1H), 9.35 (br, 1H), 10.24 (d, *J* =4.0Hz, 1H). MS (ESI) m/z = 571.1693 ($M+H^+$), calcd. for $C_{27}H_{26}ClF_2N_6O_4$ m/z = 571.1672.

*5.5. General method for preparing of analogs **13a-j***

*5.5.1. N-(4-((3,4-difluorophenyl)amino)-7-(3-morpholinopropoxy)quinazolin-6-yl)-2-fluoro-5-nitrobenzamide (**13a**)*

Pale yellow solid; yield: 32%. ^{1}H NMR (400 MHz, DMSO-d_6) δ 2.24-2.30 (m, 2H), 3.07-3.13 (m, 2H), 3.37-3.41 (m, 2H), 3.48-3.51 (m, 2H), 3.64-3.70 (m, 2H), 3.99-4.03 (m, 2H), 4.38 (t, *J* = 5.6Hz, 2H), 7.41 (s, 1H), 7.49-7.54 (m, 1H), 7.58-7.61 (m, 1H), 7.76 (t, *J* = 9.2Hz, 1H), 7.98-8.03 (m, 1H), 8.52-8.56 (m, 1H),

8.64 (dd, *J* = 3.2, 6.0Hz, 1H), 8.71 (s, 1H), 9.03 (m, 1H), 9.93 (br, 1H), 10.28 (d, *J* = 3.6Hz, 1H). MS (ESI) m/z = 583.1926 ($M+H^+$), calcd. for $C_{28}H_{25}F_3N_6O_5$ m/z = 583.1917.

*5.5.2. 2-fluoro-N-(4-((4-fluorophenyl)amino)-7-(3-morpholinopropoxy)quinazolin-6-yl)-5-nitrobenzamide (**13b**)*

Pale yellow solid; yield: 26%. ^{1}H NMR (400 MHz, DMSO-d_6) δ 2.24-2.29 (m, 2H), 3.05-3.13 (m, 2H), 3.39 (m, 2H), 3.37-3.41 (m, 2H), 3.48-3.51 (m, 2H), 3.67 (t, *J* = 12.0Hz, 2H), 3.99-4.03 (m, 2H), 4.38 (t, *J* = 5.6Hz, 2H), 7.27-7.32 (m, 2H), 7.39 (s, 1H), 7.73-7.78 (m, 3H), 8.52-8.56 (m, 1H), 8.63 (dd, *J* = 3.2, 6.0Hz, 1H), 8.71 (s, 1H), 9.06 (s, 1H), 9.91 (br, 1H), 10.30 (d, *J* = 3.2Hz, 1H). MS (ESI) m/z = 565.2027 ($M+H^+$), calcd. for $C_{28}H_{26}F_2N_6O_5$ m/z = 565.2011.

*5.5.3. N-(4-((3-chloro-4-cyanophenyl)amino)-7-(3-morpholinopropoxy)quinazolin-6-yl)-2-fluoro-5-nitrobenzamide (**13c**)*

Pale yellow solid; yield: 29%. ^{1}H NMR (400 MHz, DMSO-d_6) δ 1.98-2.02 (m, 2H), 2.37 (bs, 4H), 3.29 (m, 2H), 3.56-3.58 (m, 4H), 4.32 (t, *J* = 6.0Hz, 2H), 7.41 (s, 1H), 7.75 (t, *J* = 9.2Hz, 1H), 7.95 (d, *J* = 8.8Hz, 1H), 8.10 (dd, *J* = 2.0, 8.8Hz, 1H), 8.42 (d, *J* = 2.0Hz, 1H), 8.50-8.53 (m, 1H), 8.61-8.64 (m, 1H), 8.72 (s, 1H), 8.98 (s, 1H), 10.19 (d, *J* =4.0 Hz, 1H), 10.24 (s, 1H). MS (ESI) m/z 606.1674 ($M+H^+$), calcd. for $C_{29}H_{26}ClFN_7O_5$ m/z = 606.1668.

*5.5.4. N-(4-((3-chloro-4-(cyclopropylmethoxy)phenyl)amino)-7-(3-morpholinopropoxy)quinazolin-6-yl)-2-fluoro-5-nitrobenzamide (**13d**)*

Pale yellow solid; yield: 30%. ^{1}H NMR (400 MHz, DMSO-d_6) δ 0.35-0.39 (m, 2H), 0.58-0.63 (m, 2H), 1.23-1.29 (m, 1H), 2.26 (m, 2H), 3.10 (m, 2H), 3.40 (d, *J* = 8.0Hz, 2H), 3.70 (m, 2H), 3.96 (d, *J* = 6.8Hz, 2H), 4.01 (m, 2H), 4.37 (t, *J* = 5.6Hz, 2H), 7.20 (d, *J* = 9.2Hz, 1H), 7.42 (s, 1H), 7.62 (dd, *J* = 2.8, 9.2Hz, 1H), 7.75 (t, *J* = 9.2Hz, 1H), 7.88 (d, *J* = 2.8Hz, 1H), 8.52-8.56 (m, 1H), 8.63 (dd, *J* = 2.8, 6.0Hz, 1H), 8.74 (s, 1H), 9.06 (s, 1H), 10.30 (d, *J* = 3.6Hz, 1H), 10.70 (s, 1H). MS (ESI) m/z = 651.2152 ($M+H^+$), calcd. for $C_{32}H_{33}ClFN_6O_6$ m/z = 651.2134. ^{13}C NMR (100 MHz, DMSO-d_6) δ 3.12, 10.07, 22.80, 51.33, 53.34, 63.39, 66.23, 73.35, 107.83, 113.92, 117.84, 118.43, 120.86, 123.66, 124.30, 125.37, 126.08, 127.10, 128.80, 131.23, 144.00, 151.45, 152.29, 155.61, 158.00, 158.40, 160.64, 161.46, 164.04.

*5.5.5. N-(4-((3-chloro-4-(2-methoxyethoxy)phenyl)amino)-7-(3-morpholinopropoxy)quinazolin-6-yl)-2-fluoro-5-nitrobenzamide (**13e**)*

Pale yellow solid; yield: 33%. ^{1}H NMR (400 MHz, DMSO-d_6) δ 2.28 (m, 2H), 3.10 (m, 2H), 3.36 (s, 3H), 3.41 (m, 2H), 3.50 (m, 2H), 3.72 (m, 4H), 4.00 (m, 2H), 4.23 (m, 2H), 4.38 (t, *J* = 5.6Hz, 2H), 7.26 (d, *J* = 9.2Hz, 1H), 7.47 (s, 1H), 7.62 (dd, *J* = 2.8, 8.8Hz, 1H), 7.75 (t, *J* = 9.2Hz, 1H), 7.85 (d, *J* = 2.4Hz, 1H), 8.51-8.56 (m, 1H), 8.64 (dd, *J* = 2.8, 6.0Hz, 1H), 8.83 (s, 1H), 9.13 (s, 1H), 10.35 (d, *J* = 3.6Hz, 1H), 11.05 (s, 1H). MS (ESI) m/z = 655.2081 ($M+H^+$), calcd. for $C_{31}H_{33}ClFN_6O_7$ m/z = 655.2083. ^{13}C NMR (100 MHz, DMSO-d_6) δ 22.76, 51.31, 53.30, 58.39, 63.36, 66.40, 68.54, 70.25, 107.44, 113.73, 117.88, 118.42, 120.82, 124.18, 124.33, 125.91, 126.08, 127.54, 128.83, 130.81, 144.00, 151.48, 151.80, 155.98, 158.37, 158.39, 160.69, 161.47, 164.05.

*5.5.6. N-(4-((3-chloro-4-(2-(dimethylamino)ethoxy)phenyl)amino)-7-(3-morpholinopropoxy) quinazolin-6-yl)-2-fluoro-5-nitrobenzamide (**13f**)*

Pale yellow solid; yield: 31%. ^{1}H NMR (400 MHz, DMSO-d_6) δ 2.24-2.33 (m, 2H), 2.94 (s, 3H), 2.95 (s, 3H), 3.07-3.12 (m, 2H), 3.36-3.39 (m, 4H), 3.60-3.67 (m, 4H), 4.00-4.03 (m, 2H), 4.37 (t, *J* = 5.6Hz, 2H), 4.44 (t, *J* = 4.8Hz, 2H), 7.30 (d, *J* = 9.2Hz, 1H), 7.39 (s, 1H), 7.71 (dd, *J* = 2.4, 9.2Hz, 1H), 7.76 (t, *J* = 9.2Hz, 1H), 7.97 (d, *J* = 2.4Hz, 1H), 8.52-8.56 (m, 1H), 8.63 (dd, *J* = 3.2, 6.0Hz, 1H), 8.67 (s, 1H), 9.02 (s, 1H), 9.75 (br, 1H), 10.28 (d, *J* = 3.2Hz, 1H). MS (ESI) m/z = 668.2398 ($M+H^+$), calcd. for $C_{32}H_{36}ClFN_7O_6$ m/z = 668.2400.

*5.5.7. 2-fluoro-N-(4-((3-chloro-4-((6-methylpyridin-3-yl)oxy)phenyl)amino)-7-(3-morpholinopropoxy)quinazolin-6-yl)-5-nitrobenzamide (**13g**)*

Pale yellow solid; yield: 38%. ^{1}H NMR (400 MHz, DMSO-d_6) δ 2.26-2.32 (m, 2H), 2.49 (s, 3H), 3.07-3.13 (m, 2H), 3.41 (t, *J* = 8.0Hz, 2H), 3.49-3.51 (m, 2H), 3.97-4.02 (m, 4H), 4.39 (t, *J* = 5.6Hz, 2H), 7.25 (d, *J* = 8.8Hz, 1H), 7.36-7.38 (m, 1H), 7.42-7.46 (m, 2H), 7.73-7.78 (m, 2H), 8.11 (d, *J* = 2.4Hz, 1H), 8.31 (d, *J* = 2.8Hz, 1H), 8.52-8.56 (m, 1H), 8.64 (dd, *J* = 2.8, 6.0Hz, 1H), 8.84 (s, 1H), 9.13 (s, 1H), 10.14 (br, 1H), 10.35 (d, *J* = 3.2Hz, 1H). MS (ESI) m/z 688.2094 ($M+H^+$), calcd. for $C_{34}H_{32}ClFN_7O_6$ m/z = 688.2087.

*5.5.8. N-(4-((3-chloro-4-(3-cyanophenoxy)phenyl)amino)-7-(3-morpholinopropoxy)quinazolin-6-yl)-2-fluoro-5-nitrobenzamide (**13h**)*

Pale yellow solid; yield: 34%. ^{1}H NMR (400 MHz, DMSO-d_6) δ 2.26-2.30 (m, 2H), 3.06-3.13 (m, 4H), 3.65-3.72 (m, 4H), 3.99-4.02(m, 2H), 4.39 (t, *J* = 6.0Hz, 2H), 7.29-7.33 (m, 1H), 7.35 (s, 1H), 7.41 (s, 1H), 7.48 (d, *J* = 2.4Hz, 1H), 7.60-7.62 (m, 2H), 7.76 (t, *J* = 9.2Hz, 1H), 7.85 (dd, *J* = 2.4, 9.2Hz, 1H), 8.19 (m, 1H), 8.52-8.56 (m, 1H), 8.64 (dd, *J* = 3.2, 6.0Hz, 1H), 8.75 (s, 1H), 9.06 (s, 1H), 9.96 (br, 1H), 10.29 (d, *J* = 3.6Hz, 1H). MS (ESI) m/z = 698.1926 ($M+H^+$), calcd. for $C_{35}H_{30}FN_7O_6$ m/z = 698.1930.

*5.5.9. N-(4-((3-chloro-4-(pyridin-2-ylmethoxy)phenyl)amino)-7-(3-morpholinopropoxy)quinazolin-6-yl)-2-fluoro-5-nitrobenzamide (**13i**)*

Pale yellow solid; yield: 33%. ^{1}H NMR (400 MHz, DMSO-d_6) δ 2.25-2.29 (m, 2H), 3.06-3.12 (m, 4H), 3.64-3.71 (m, 4H), 3.98-4.03 (m, 2H), 4.38 (t, *J* = 5.6Hz, 2H), 5.33 (s, 2H), 7.33 (d, *J* = 8.8Hz, 1H), 7.38-7.41 (m, 2H), 7.59-7.64 (m, 2H), 7.76 (t, *J* = 9.2Hz, 1H), 7.88-7.93 (m, 2H), 8.52-8.56 (m, 1H), 8.60-8.65 (m, 2H), 8.78 (s, 1H), 9.07 (s, 1H), 9.96 (br, 1H), 10.32 (d, *J* = 3.2Hz, 1H). MS (ESI) m/z = 688.2089 ($M+H^+$), calcd. for $C_{34}H_{32}ClFN_7O_6$ m/z = 688.2087.

*5.5.10. N-(4-((3-chloro-4-((3-fluorobenzyl)oxy)phenyl)amino)-7-(3-morpholinopropoxy)quinazolin-6-yl)-2-fluoro-5-nitrobenzamide (**13j**)*

Pale yellow solid; yield: 32%. ^{1}H NMR (400 MHz, DMSO-d_6) δ 2.23-2.29 (m, 2H), 3.06-3.12 (m, 4H), 3.64-3.71 (m, 4H), 3.98-4.04 (m, 2H), 4.37 (t, *J* = 5.6Hz, 2H), 5.28 (s, 2H), 7.16-7.22 (m, 1H), 7.29-7.35 (m, 3H), 7.37 (s, 1H), 7.45-7.51 (m, 1H), 7.65 (dd, *J* = 2.4, 8.8Hz, 1H), 7.76 (t, *J* = 9.2Hz, 1H), 7.93 (d, *J* = 2.8Hz, 1H), 8.52-8.56 (m, 1H), 8.63 (dd, *J* = 2.8, 6.0Hz, 1H), 8.70 (s, 1H), 9.02 (s, 1H), 9.85 (br, 1H), 10.28 (s, 1H). MS (ESI) m/z = 705.2069 ($M+H^+$), calcd. for $C_{35}H_{32}ClF_2N_6O_6$ m/z = 705.2040.

5.6. EGFR kinase inhibition assay

The cell culture reagents RPMI1640, DMEM, FBS were purchased from Invitrogen (life technologies). The EGFR proteins were purchased from Carna Bioscience. The HTRF KinEASE-TK kit (Cat# 62TK0PEC) was from Cisbio. The Cell Titer-Glo Luminescent Cell Viability Assay kit (Cat# G7573) was purchased from Promega. All the other chemicals were from Sigma. The assay and cell culture plates were purchased from Corning.

The EGFR kinase assays were performed in 384-well plate (Corning 3676, low volume, black, NBS), using Cisbio HTRF KinEASE-TK kit. The assay buffer contained 50mM HEPES (pH7.0), 0.02% NaN_3, 0.01% BSA, 0.1mM Orthovanadate,

10mM $MgCl_2$, 2.5mM DTT and 6.25nM SEB. EGFR kinases was first incubated with compounds for 2h respectively, then ATP/Peptide substrate mixture was added to initiate the reaction. The final concentration EGFR WT was 0.1nM, EGFR d746-750 and EGFR L858R and EGFR L858R/T790M were 0.06nM. The final concentration of biotin-labeled peptide substrate was 1.4μM, and ATP was 20μM for EGFR WT, 100μM for EGFR d746-750 and EGFR L858R. After 30min reaction at room temperature, the detection reagents were added. The TR-FRET signal was measured on PerkinElmer Envision using excitation 320nm and emission 615nm/665nm. The data was analyzed using Graphpad Prism (GraphPad Software; www.graphpad.com). The curves were fitted using a non-linear regression model with a sigmoidal dose response.

5.7. Cell culture and cell survival assay

Ba/F3 (EGFR L858R), Ba/F3 (EGFR Del E746_A750), Ba/F3 (cat-EGFR), and Ba/F3 (Her2 negative) stable cell lines were kindly provided by Dr. Chen Liang from Jinan University. Cancer cell lines A431, HCC827 and NCI-H1975 were purchased from ATCC. All cells were cultured in RPMI-1640 medium (Hyclone, Logan, UT), supplemented with 10% FBS (Invitrogen) and 100 units/ml penicillin/streptomycin (Hyclone). Cells were maintained at 37°C in humidified atmosphere of 5% CO_2.

Cancer cells or Ba/F3 cells were plated in 384-well cell culture plate (Corning 3570), and exposed to compounds treatment for 72 hours. Cell survival analysis was performed using the Cell Titer-Glo Luminescent Cell Viability Assay kit (Promega) following manufactory instruction with minor modification. In brief, 20 μl of Cell Titer-glo reagent was added to the 30μl cell culture medium. Cell culture plates were place on a shaker for 10 min and were then incubated at room temperature for an additional 10 min. Luminescent reading was carried on Enspire (PerkinElmer).

5.8. Western blotting

A431 cells were seeded to 6-well plate on day1 and on day2 replace with new medium. The cells were treated with CI-1033, gefitinib, or **6g** respectively for 1 hour, then either immediately treated with EGF for 15min or thoroughly washed with fresh medium 3 times for 8h before EGF treatment. Cells was collected and re-suspended with lysis buffer (20 mM Tris-HCl, pH 7.4, 150 mM NaCl, 10% glycerol, 1% Triton X-100, 1 mM Na_3VO_4, 25 mM ß-glycerol-phosphate, 0.1mM PMSF, complete protease inhibitor cocktail phosphatase inhibitor cocktail(Roche)). The re-suspended cell pellet was incubated on ice for 30 min and centrifuged at 15,000 g for 10 min. The supernatants were collected for western-blot analysis.

5.9. Compounds stability test in liver microsome assays

Compound **6g** were incubated with human, rat or mouse liver microsomes, and reactions were initiated by the addition of NADPH in 0.05 M Phosphate buffer (pH=7.4) at 37°C for 0-60 min. The reaction was quenched, and the amount of the remaining compound was analyzed using LC-MS/MS.

5.10. Pharmacokinetics study in mice

Following oral administration (PO) of **6g** to C57BL/6 mice (n = 3), blood sample was collected at various time points. The concentrations of the compound in plasma samples were measured by LC-MS/MS. Pharmacokinetic parameters were determined using noncompartmental analysis in phoenix 64 (winNonlin 6.3).

5.11. Molecular docking

The molecular docking was performed using MOE 2015.10 software. The co-crystal structure of EGFR T790M in complex with BIBW2992 (PDB ID:4G5P) was used for docking studies. The optimized structure of **6g** was generated by MOE 2015.10. Before docking simulation, ligands and protein were prepared with the standard protocol using MOE 2015.10. **6g** was inserted into the ATP-binding pocket of EGFR T790M to replace BIBW2992. The complex of **6g**-EGFR was used for geometrical optimization. All docking calculations were performed using default settings.

Acknowledgments

We thank Dr. Liang Chen (Jinan University) for the Ba/F3 cell lines. We thank Mr. Yupeng Wang for his help of several compounds synthesis. This work was supported by the National High Technology Project 973 (2011CB504300).

References and notes

1. Yarden, Y. The EGFR family and its ligands in human cancer. *Eur. J. Cancer* **2001,** 37: 3-8.
2. Woodburn, J. R. The Epidermal Growth Factor Receptor and Its Inhibition in Cancer Therapy. *Pharmacol. Ther.* **1999,** 82: 241-250.
3. Tu, Y.; Wang, C.; Xu, S.; Lan, Z.; Li, W.; Han, J.; Zhou, Y.; Zheng, P.; Zhu, W. Design, synthesis, and docking studies of quinazoline analogues bearing aryl semicarbazone scaffolds as potent EGFR inhibitors. *Biorg. Med. Chem.* **2017,** 25: 3148-3157.
4. Yarden, Y.; Sliwkowski, M. X. Untangling the ErbB signalling network. *Nat. Rev. Mol. Cell Biol.* **2001,** 2: 127-137.
5. Govindan, R. A Review of Epidermal Growth Factor Receptor/HER2 Inhibitors in the Treatment of Patients With Non–Small-Cell Lung Cancer. *Clin. Lung. Cancer* **2010,** 11: 8-12.
6. Irish, J. C.; Bernstein, A. Oncogenes in head and neck cancer. *The Laryngoscope* **1993,** 103: 42-52.
7. Moscatello, D. K.; Holgado-Madruga, M.; Godwin, A. K.; Ramirez, G.; Gunn, G.; Zoltick, P. W.; Biegel, J. A.; Hayes, R. L.; Wong, A. J. Frequent Expression of a Mutant Epidermal Growth Factor Receptor in Multiple Human Tumors. *Cancer Res.* **1995,** 55: 5536.
8. Nicholson, R. I.; Gee, J. M. W.; Harper, M. E. EGFR and cancer prognosis. *Eur. J. Cancer* **2001,** 37: 9-15.
9. Barker, A. J.; Gibson, K. H.; Grundy, W.; Godfrey, A. A.; Barlow, J. J.; Healy, M. P.; Woodburn, J. R.; Ashton, S. E.; Curry, B. J.; Scarlett, L.; Henthorn, L.; Richards, L. Studies leading to the identification of ZD1839 (iressa™): an orally active, selective epidermal growth factor receptor tyrosine kinase inhibitor targeted to the treatment of cancer. *Bioorg. Med. Chem. Lett.* **2001,** 11: 1911-1914.
10. Han, S.-W.; Kim, T.-Y.; Hwang, P. G.; Jeong, S.; Kim, J.; Choi, I. S.; Oh, D.-Y.; Kim, J. H.; Kim, D.-W.; Chung, D. H.; Im, S.-A.; Kim, Y. T.; Lee, J. S.; Heo, D. S.; Bang, Y.-J.; Kim, N. K. Predictive and Prognostic Impact of Epidermal Growth Factor Receptor Mutation in Non–Small-Cell Lung Cancer Patients Treated With Gefitinib. *J. Clin. Oncol.* **2005,** 23: 2493-2501.
11. Dai, Q.; Ling, Y.-H.; Lia, M.; Zou, Y.-Y.; Kroog, G.; Iwata, K. K.; Perez-Soler, R. Enhanced Sensitivity to the HER1/Epidermal Growth Factor Receptor Tyrosine Kinase Inhibitor Erlotinib Hydrochloride in Chemotherapy-Resistant Tumor Cell Lines. *Clin. Cancer. Res.* **2005,** 11: 1572.
12. Melosky, B.; Agulnik, J.; Assi, H. Retrospective practice review of treatment of metastatic non-small-cell lung cancer with second-line erlotinib. *Current Oncology* **2008,** 15: 279-285.
13. Xiao, Q.; Qu, R.; Gao, D.; Yan, Q.; Tong, L.; Zhang, W.; Ding, J.; Xie, H.; Li, Y. Discovery of 5-(methylthio)pyrimidine derivatives as L858R/T790M mutant selective epidermal growth factor receptor (EGFR) inhibitors. *Biorg. Med. Chem.* **2016,** 24: 2673-2680.
14. Engelman, J. A.; Jänne, P. A. Mechanisms of Acquired Resistance to Epidermal Growth Factor Receptor Tyrosine Kinase Inhibitors in Non–Small Cell Lung Cancer. *Clin. Cancer. Res.* **2008,** 14: 2895-2899.
15. Pao, W.; Miller, V. A.; Politi, K. A.; Riely, G. J.; Somwar, R.; Zakowski, M. F.; Kris, M. G.; Varmus, H. Acquired Resistance of Lung Adenocarcinomas to Gefitinib or Erlotinib Is Associated with a Second Mutation in the EGFR Kinase Domain. *PLoS Med.* **2005,** 2: e73.
16. Kobayashi, S.; Boggon, T. J.; Dayaram, T.; Jänne, P. A.; Kocher, O.; Meyerson, M.; Johnson, B. E.; Eck, M. J.; Tenen, D. G.; Halmos, B. EGFR mutation and resistance of non–small-cell lung cancer to gefitinib. *New Engl. J. Med.* **2005,** 352: 786-792.

17. Engelman, J. A.; Jänne, P. A. Mechanisms of Acquired Resistance to Epidermal Growth Factor Receptor Tyrosine Kinase Inhibitors in Non–Small Cell Lung Cancer. *Clin. Cancer. Res.* **2008,** 14: 2895.
18. Kwak, E. L.; Sordella, R.; Bell, D. W.; Godin-Heymann, N.; Okimoto, R. A.; Brannigan, B. W.; Harris, P. L.; Driscoll, D. R.; Fidias, P.; Lynch, T. J.; Rabindran, S. K.; McGinnis, J. P.; Wissner, A.; Sharma, S. V.; Isselbacher, K. J.; Settleman, J.; Haber, D. A. Irreversible inhibitors of the EGF receptor may circumvent acquired resistance to gefitinib. *Proc. Natl. Acad. Sci. U. S. A.* **2005,** 102: 7665-7670.
19. Basu, D.; Richters, A.; Rauh, D. Structure-based design and synthesis of covalent-reversible inhibitors to overcome drug resistance in EGFR. *Biorg. Med. Chem.* **2015,** 23: 2767-2780.
20. Gao, H.; Yang, Z.; Yang, X.; Rao, Y. Synthesis and evaluation of osimertinib derivatives as potent EGFR inhibitors. *Biorg. Med. Chem.* **2017,** 25: 4553-4559.
21. Ji, X.; Peng, T.; Zhang, X.; Li, J.; Yang, W.; Tong, L.; Qu, R.; Jiang, H.; Ding, J.; Xie, H.; Liu, H. Design, synthesis and biological evaluation of novel 6-alkenylamides substituted of 4-anilinothieno[2,3-d]pyrimidines as irreversible epidermal growth factor receptor inhibitors. *Biorg. Med. Chem.* **2014,** 22: 2366-2378.
22. Dungo, R. T.; Keating, G. M. Afatinib: First Global Approval. *Drugs* **2013,** 73: 1503-1515.
23. Greig, S. L. Osimertinib: First Global Approval. *Drugs* **2016,** 76: 263-273.
24. Kim, E. S. Olmutinib: First Global Approval. *Drugs* **2016,** 76: 1153-1157.
25. Carmi, C.; Lodola, A.; Rivara, S.; Vacondio, F.; Cavazzoni, A.; R. Alfieri, R.; Ardizzoni, A.; G. Petronini, P.; Mor, M. Epidermal Growth Factor Receptor Irreversible Inhibitors: Chemical Exploration of the Cysteine-Trap Portion. *Mini-Rev. Med. Chem.* **2011,** 11: 1019-1030.
26. Carmi, C.; Cavazzoni, A.; Vezzosi, S.; Bordi, F.; Vacondio, F.; Silva, C.; Rivara, S.; Lodola, A.; Alfieri, R. R.; La Monica, S.; Galetti, M.; Ardizzoni, A.; Petronini, P. G.; Mor, M. Novel Irreversible Epidermal Growth Factor Receptor Inhibitors by Chemical Modulation of the Cysteine-Trap Portion. *J. Med. Chem.* **2010,** 53: 2038-2050.
27. Carmi, C.; Galvani, E.; Vacondio, F.; Rivara, S.; Lodola, A.; Russo, S.; Aiello, S.; Bordi, F.; Costantino, G.; Cavazzoni, A.; Alfieri, R. R.; Ardizzoni, A.; Petronini, P. G.; Mor, M. Irreversible Inhibition of Epidermal Growth Factor Receptor Activity by 3-Aminopropanamides. *J. Med. Chem.* **2012,** 55: 2251-2264.
28. Sanger, F. The free amino groups of insulin. *Biochem. J* **1945,** 39: 507-515.
29. Chen, K. X.; Lesburg, C. A.; Vibulbhan, B.; Yang, W.; Chan, T.-Y.; Venkatraman, S.; Velazquez, F.; Zeng, Q.; Bennett, F.; Anilkumar, G. N.; Duca, J.; Jiang, Y.; Pinto, P.; Wang, L.; Huang, Y.; Selyutin, O.; Gavalas, S.; Pu, H.; Agrawal, S.; Feld, B.; Huang, H.-C.; Li, C.; Cheng, K.-C.; Shih, N.-Y.; Kozlowski, J. A.; Rosenblum, S. B.; Njoroge, F. G. A Novel Class of Highly Potent Irreversible Hepatitis C Virus NS5B Polymerase Inhibitors. *J. Med. Chem.* **2012,** 55: 2089-2101.
30. Solca, F.; Dahl, G.; Zoephel, A.; Bader, G.; Sanderson, M.; Klein, C.; Kraemer, O.; Himmelsbach, F.; Haaksma, E.; Adolf, G. R. Target Binding Properties and Cellular Activity of Afatinib (BIBW 2992), an Irreversible ErbB Family Blocker. *J. Pharmacol. Exp. Ther.* **2012,** 343: 342.
31. Tsou, H.-R.; Mamuya, N.; Johnson, B. D.; Reich, M. F.; Gruber, B. C.; Ye, F.; Nilakantan, R.; Shen, R.; Discafani, C.; DeBlanc, R.; Davis, R.; Koehn, F. E.; Greenberger, L. M.; Wang, Y.-F.; Wissner, A. 6-Substituted-4-(3-bromophenylamino)quinazolines as Putative Irreversible Inhibitors of the Epidermal Growth Factor Receptor (EGFR) and Human Epidermal Growth Factor Receptor (HER-2) Tyrosine Kinases with Enhanced Antitumor Activity. *J. Med. Chem.* **2001,** 44: 2719-2734.
32. Albanell, J.; Rojo, F.; Averbuch, S.; Feyereislova, A.; Mascaro, J. M.; Herbst, R.; LoRusso, P.; Rischin, D.; Sauleda, S.; Gee, J.; Nicholson, R. I.; Baselga, J. Pharmacodynamic Studies of the Epidermal Growth Factor Receptor Inhibitor ZD1839 in Skin From Cancer Patients: Histopathologic and Molecular Consequences of Receptor Inhibition. *J. Clin. Oncol.* **2002,** 20: 110-124.
33. Segaert, S.; Van Cutsem, E. Clinical signs, pathophysiology and management of skin toxicity during therapy with epidermal growth factor receptor inhibitors. *Ann. Oncol.* **2005,** 16: 1425-1433.
34. Hirsh, V.; Blais, N.; Burkes, R.; Verma, S.; Croitoru, K. Management of diarrhea induced by epidermal growth factor receptor tyrosine kinase inhibitors. *Current Oncology* **2014,** 21: 329-336.
35. Shepherd, F. A.; Rodrigues Pereira, J.; Ciuleanu, T.; Tan, E. H.; Hirsh, V.; Thongprasert, S.; Campos, D.; Maoleekoonpiroj, S.; Smylie, M.; Martins, R.; van Kooten, M.; Dediu, M.; Findlay, B.; Tu, D.; Johnston, D.; Bezjak, A.; Clark, G.; Santabárbara, P.; Seymour, L. Erlotinib in Previously Treated Non–Small-Cell Lung Cancer. *New Engl. J. Med.* **2005,** 353: 123-132.
36. Yamamoto, N.; Honma, M.; Suzuki, H. Off-Target Serine/Threonine Kinase 10 Inhibition by Erlotinib Enhances Lymphocytic Activity Leading to Severe Skin Disorders. *Mol. Pharmacol*. **2011,** 80: 466.
37. Kitagawa, D.; Yokota, K.; Gouda, M.; Narumi, Y.; Ohmoto, H.; Nishiwaki, E.; Akita, K.; Kirii, Y. Activity - based kinase profiling of approved tyrosine kinase inhibitors. *Genes Cells* **2013,** 18: 110-122.
38. Traxler, P. M.; Furet, P.; Mett, H.; Buchdunger, E.; Meyer, T.; Lydon, N. 4-(Phenylamino)pyrrolopyrimidines: Potent and Selective, ATP Site Directed Inhibitors of the EGF-Receptor Protein Tyrosine Kinase. *J. Med. Chem.* **1996,** 39: 2285-2292.
39. Fabbro, D.; Ruetz, S.; Buchdunger, E.; Cowan-Jacob, S. W.; Fendrich, G.; Liebetanz, J.; Mestan, J.; O'Reilly, T.; Traxler, P.; Chaudhuri, B.; Fretz, H.; Zimmermann, J.; Meyer, T.; Caravatti, G.; Furet, P.; Manley, P. W. Protein kinases as targets for anticancer agents: from inhibitors to useful drugs. *Pharmacol. Ther.* **2002,** 93: 79-98.
40. Zhou, W.; Ercan, D.; Chen, L.; Yun, C.-H.; Li, D.; Capelletti, M.; Cortot, A. B.; Chirieac, L.; Iacob, R. E.; Padera, R.; Engen, J. R.; Wong, K.-K.; Eck, M. J.; Gray, N. S.; Janne, P. A. Novel mutant-selective EGFR kinase inhibitors against EGFR T790M. *Nature* **2009,** 462: 1070-1074.
41. Finlay, M. R. V.; Anderton, M.; Ashton, S.; Ballard, P.; Bethel, P. A.; Box, M. R.; Bradbury, R. H.; Brown, S. J.; Butterworth, S.; Campbell, A.; Chorley, C.; Colclough, N.; Cross, D. A. E.; Currie, G. S.; Grist, M.; Hassall, L.; Hill, G. B.; James, D.; James, M.; Kemmitt, P.; Klinowska, T.; Lamont, G.; Lamont, S. G.; Martin, N.; McFarland, H. L.; Mellor, M. J.; Orme, J. P.; Perkins, D.; Perkins, P.; Richmond, G.; Smith, P.; Ward, R. A.; Waring, M. J.; Whittaker, D.; Wells, S.; Wrigley, G. L. Discovery of a Potent and Selective EGFR Inhibitor (AZD9291) of Both Sensitizing and T790M Resistance Mutations That Spares the Wild Type Form of the Receptor. *J. Med. Chem.* **2014,** 57: 8249-8267.
42. Boelsterli, U. A.; Ho, H. K.; Zhou, S.; Yeow Leow, K. Bioactivation and Hepatotoxicity of Nitroaromatic Drugs. *Curr. Drug Metab.* **2006,** 7: 715-727.
43. Mortelmans, K.; Zeiger, E. The Ames Salmonella/microsome mutagenicity assay. *Mutation Research/Fundamental and Molecular Mechanisms of Mutagenesis* **2000,** 455: 29-60.